Hindawi
Journal of Nanomaterials
Volume 2022, Article ID 7086199, 12 pages
https://doi.org/10.1155/2022/7086199

Research Article

Construction of MPEG-PCL Nanomicelle Ocular Drug Delivery Vector and Its Application in the Treatment of Hypertensive Fundus Disease

Hongxiao Xu,[1] Jingxing Liu,[2] Zhaoxia Teng,[3] Ming Ru,[1] Zhaoping Wang,[4] and Yingcui Wang[1]

[1]*Department of Cardiology, Qilu Hospital (Qingdao), Cheeloo College of Medicine, Shandong University, Qingdao, 266035 Shandong, China*
[2]*Emergency Department, Qingdao Municipal Hospital (Group), Qingdao NO.9 People's Hospital, Qingdao, 266000 Shandong, China*
[3]*Department of Endocrinology, Qingdao Municipal Hospital (Group), Qingdao NO.9 People's Hospital, Qingdao, 266000 Shandong, China*
[4]*Department of Emergency, Qilu Hospital (Qingdao), Cheeloo College of Medicine, Shandong University, Qingdao, 266035 Shandong, China*

Correspondence should be addressed to Zhaoping Wang; wang_zp2008@163.com
and Yingcui Wang; 199462000803@email.sdu.edu.cn

Received 10 January 2022; Revised 9 February 2022; Accepted 21 February 2022; Published 18 March 2022

Academic Editor: Awais Ahmed

With the continuous development of society and the continuous development of technology, people's living standards have gradually improved, and the development of new things has gradually entered a new agenda. Alcoholism has gradually taken over most people's lives. Excessive drinking can lead to excessive alcohol content in the body, which is harmful to the liver. The stomach and other organs are affected, and the formation of high blood pressure is directly related to excessive drinking. And hypertensive patients are prone to have some adverse reactions and cause other more serious diseases. Hypertensive ocular fundus disease is one of its complications. Hypertensive ophthalmopathy is caused by abnormal changes in the retina, which can be very harmful. Patients with low rates and blindness can cause vision loss. Such diseases must be treated in time to allow patients to get rid of the troubles of the disease as soon as possible and restore their quality of life. In the treatment of hypertensive fundus disease, low-intensity laser radiation combined with nanomicelle ocular drug delivery carrier treatment has achieved a relatively ideal treatment effect. This article adopts the comparative treatment method and selects 120 patients with hypertensive ocular fundus disease admitted to X Hospital from 2018 to 2020 and evenly distributes them into the experimental group and the control group for comparative treatment experiments. Conclusions are obtained based on the analysis of treatment data. Related factors analyzed include age, gender, whether retinal laser photocoagulation has been performed before, and whether anti-VEGF treatment has been performed before surgery. The experimental results proved that there was no difference in the overall quality of life between the two groups before the treatment and at the end of the first course of treatment ($P > 0.05$), and the overall quality of life of the experimental group was higher than that of the control group until the end of the second course of treatment ($P < 0.05$). Hypertensive fundus disease is very harmful. If it is not treated in time, it will cause blindness in patients. In the treatment of hypertensive fundus disease, the use of low-intensity laser irradiation combined with MPEG-PCL nanomicelle therapy is beneficial to the recovery of vision and blood flow. The change index can guarantee the safety of treatment at the same time, which is worthy of clinical promotion.

1. Introduction

Ophthalmic diseases have more complex causes, more different diseases, and more variable conditions and belong to clinical ophthalmic diseases. It will seriously affect the vision of the patient and may even cause blindness. Therefore, in order to effectively improve the vision of patients, the abovementioned various consequences must be effectively prevented. Effective treatment of patients with bottom disease is very important. The traditional method of administration can make the drug concentration in the retina reach a higher level, but the half-life of the drug in the vitreous is shorter. Therefore, chronic uveitis requires repeated injections and patient compliance is poor. In order to solve the above problems, nanomaterials have emerged as different carriers for drugs. Compared with traditional drug delivery methods, the use of nanomaterials to distribute drugs to treat eye diseases has great advantages. Drug nanoformulations can target drug delivery, extend the time of drug action, improve drug bioavailability, and reduce drug dosage and side effects.

Researchers at home and abroad have conducted a lot of research on the problem of blood vessel retrieval in retinal images, and new methods are constantly emerging. Foreign scholars are interested in classifier methods [1, 2]. The classifier method is mainly applied in two stages. First, perform spatial connection region segmentation through a basic algorithm, and then use peripheral features to divide the selected region into blood vessels and nonvessels. The classifier design only uses the gray matter information of blood vessels, and the influence of external conditions on the segmentation results cannot be excluded. The proportion information of the segmented object can only be obtained after the segmentation is completed, and must be used in combination with other methods, and cannot be directly used in the application field of the basic segmentation algorithm. Fengping and Weixing cited the filter operator used in air road detection and designed a classifier for blood vessel segmentation [3]. GeethaRamani and Balasubramanian use teaching samples to perform machine learning to segment samples and unknown objects [4]. Rodrigues and Marengoni divided 12 groups by calculating the average value and change of the gray pixel value under the line segment with an interval of $\pi/12$ and divided into the final blood vessel segmentation method by the support vector machine method [5].

With the rapid development of the Internet of Things technology in China, various hospitals have also accelerated the construction of medical intelligence and built a hospital information system under the new situation to realize the sharing of medical information and resources, and at the same time carry out the reasonable allocation of medical resources in hospitals and communities [6–9]. The image of the retinal fundus is often affected by external conditions, resulting in problems such as uneven light, uneven contrast, and weak contrast between blood vessels and the collected image, making it difficult to remove retinal blood vessels. Haythornthwaite combines the connectivity of the blood vessel network to monitor the top line of the blood vessel to execute the structure of the blood vessel network [10], Zhang et al. proposed a segmentation threshold exploration method based on local and global features, which combines window matching and dynamics Monitoring technology is used to extract blood vessels, and iterative rules are designed, and the adaptive threshold method is further used to segment the blood vessel region. This method has achieved a good export effect [11]. Takahashi et al. monitor blood vessels by detecting the connection points and connection points of blood vessels, so as to realize network extraction [12].

The existing extraction methods are mainly aimed at normal retinal images, which are not universal. Under ideal conditions, such as uniform light distribution, less noise interference, and no disease, they can basically extract the structure of blood vessel contours correctly when diseases appear in the image, especially in large damaged areas and vascular area. This article focuses on the method of extracting blood vessels from retinal images. The purpose is to eliminate noise interference and diseases and to obtain a complete retinal blood vessel network structure. This article deeply studies the retinal blood vessels under the disease. A new technique for suppressing lesions based on a filtering method is proposed, combined with the technique of restoring the binary image of the vascular network structure, to complete the segmentation of the retinal vessel structure, thereby extracting the structure of the vessel.

2. Application of Nanomaterial Drug Delivery System in the Treatment of Hypertensive Fundus Disease

2.1. Research Content and Methods. This article first uses the literature survey method to query a large amount of data, gives a brief introduction to the preparation and characterization of nanomicelles, explains and elaborates the application of nanomaterials in medicine, and analyzes the nanomaterial drug delivery vehicle in ophthalmology treatment, the application of nanomaterials in the treatment of glaucoma, and the application of nanomaterials loaded with drugs in uveitis. After that, the method of comparative treatment was adopted, and the experimental group and the control group were compared with two different treatment methods. Here, we use the method of limiting single-factor analysis and regression analysis to analyze the influence of each factor on this experiment. Finally, based on the regression results, the construction of MPEG-PCL nanomicelle ocular drug delivery vector and its application in the treatment of hypertensive fundus disease is put forward corresponding suggestions. The article structure is shown in Figure 1.

2.2. Nanomaterials

2.2.1. Characteristics of Nanomaterials. Nanomaterials are generally very small in size, large in specific surface area, and high in surface energy. The number of surface atoms accounts for a high proportion of the total number of atoms. When the particle size is less than 10 nm, the percentage of surface atoms increases sharply, and these surface atoms

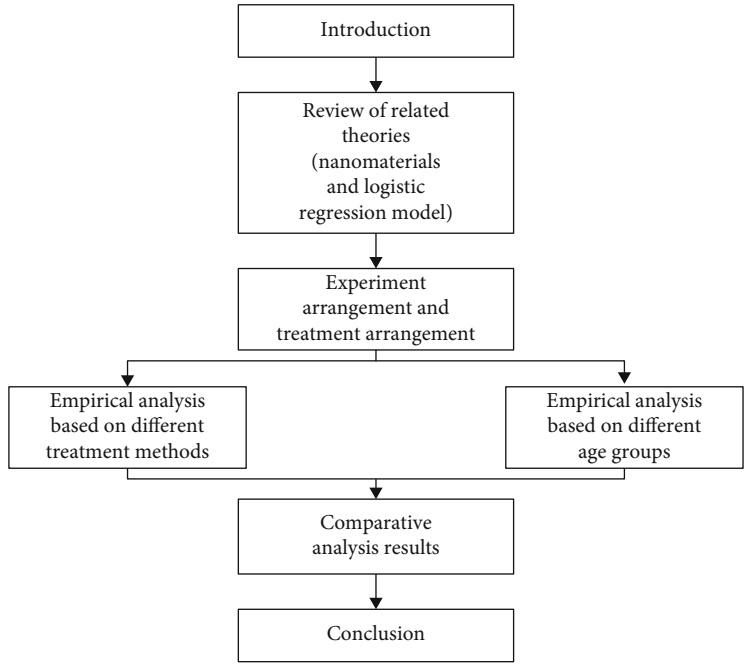

Figure 1: Research flow chart.

are in a very empty state. They have extremely high activity and are very unstable [13, 14]. Once you encounter other atoms and combine them to stabilize themselves, this effect is called surface effect.

In nanomaterials, when the particle size reaches a certain physical characteristic size, the energy levels of electrons adjacent to the metal Fermi plane change from an almost continuous state to a discrete state, while the nanoparticles have discontinuous, higher-occupancy molecules. The orbital and lower molecular orbital are asymmetry, and the energy gap is the quantum size phenomenon of nanomaterials [15].

The ability of tiny particles to pass through the dam is called the tunnel effect. When a dielectric layer with a small dielectric constant is modified on the surface of a nanomaterial, it is related to the rest of the medium surrounding the unmodified nanomaterial [16, 17]. Compared with bare nanomaterials, this will cause greater changes in its optical properties. This phenomenon is called the dielectric confinement phenomenon.

(1) Application of Nanomaterials. Throughout the scientific frontier literature and books on nanoelectrocatalysts, the most mentioned word is energy. Energy is no longer a problem of a certain country but has become a problem of global concern. When a crisis occurs, there is no one. The country can take care of itself. The vast number of scientific researchers is working against clean energy. Nanoelectrocatalysts, as a very important role in clean energy, are attracting widespread attention. Regardless of whether the heat increases or decreases, nanoelectrocatalysts will become a solution. The key to the energy problem, nanomaterials have attracted great attention since their birth [18, 19]. With the continuous advancement of science and technology, the research on nanoelectrocatalysis by scientific researchers has become more and more in-depth, and it has played its own application value in many aspects, such as hydrogen and oxygen evolution electrocatalyst, electrocatalytic carbon dioxide reduction catalyst, and microbial fuel cell electrocatalyst.

2.3. Logistic Regression Model. Regression accounting model is a two-type model, as long as the vector $x = (x_1, x_2 \cdots x_n)$ has n independent variables and the ratio coefficient is p $(y = 1|x) = p$, it can be represented by the conditional probability distribution $p(y = 1|x) = p$ of partial logistic distribution [14]. Show the observed value of $p(y = 1|x) = p$ probability. Therefore, the logistic regression model can be expressed as

$$p(y = 1 \mid x) = \pi(x) = \frac{1}{1 + e^{-g(x)}}. \tag{1}$$

Usually $f(x) = 1/1 + e^{-g(x)}$ is called the logistic function and

$$g(x) = w_0 + w_1 x_1 + \cdots + w_n x_n. \tag{2}$$

The probability that y; does not occur under the condition of x is

$$p(y = 0 \mid x) = 1 - p(y = 1 \mid x) = 1 - \frac{1}{1 + e^{-g(x)}} = \frac{1}{1 + e^{g(x)}}. \tag{3}$$

Therefore, the ratio of the probability of y occurring to not occurring is

$$\frac{p(y=1\mid x)}{p(y=0\mid x)}=\frac{p}{1-p}=e^{g(x)}. \tag{4}$$

This ratio is called the occurrence ratio of the event and is recorded as odds. Take the logarithm of odds to get

$$\ln\left(\frac{p}{1-p}\right)=g(x)=w_0+w_1x_1+\cdots+w_nx_n. \tag{5}$$

Usually use maximum likelihood estimation to find the parameters of the classification model:

$$L(w)=\prod_1^n(\pi(x_i))^{y_i}(1-\pi(x_i))^{1-y_i}. \tag{6}$$

The maximum likelihood estimation is to find the parameter $w_0, w_1, \cdots, w_n$ so that $L(w)$ takes the maximum value [20].

In the same way, the basic idea of the logistic regression model is applied to personal credit risk assessment: Given the sample data $(X_{i1}, X_{i2},\cdots,X_{\text{in}} : Y_i)(i=1,2,\cdots,k), X_i\in R^p$ of n groups of loan application customers is an indicator variable, $y_i\in[0,1]$ is a 0-1 variable, where $y_i=0$ indicates that the credit category of the i customer is a bad customer, $y_i=1$ indicates that the credit category of the i customer is a good customer [21]. The relationship between Y_i and X_{i1}, $X_{i2}\cdots X_{\text{in}}$ is as follows:

$$E(Y_i)=P_i=f(\beta_0+\beta_1X_{i1}+\beta_2X_{i2}+\cdots+\beta_nX_{\text{in}}). \tag{7}$$

Among them, $f(X)$ is a monotonically increasing function in [0,1].

$$P_i=f(X)=\frac{e^x}{1+e^x}. \tag{8}$$

Y_i is the 0-1 distribution of the mean $P_i=f(\beta_0+\beta_1X_{i1}+\beta_2X_{i2}+\cdots+\beta_nX_{\text{in}})$, the probability function:

$$\begin{aligned}P(Y_i=1)&=P_i\\P(Y_i=0)&=1-P_i\end{aligned} \tag{9}$$

Then, the logistic regression equation is

$$P_i=\frac{\exp(\beta_0+\beta_1X_{i1}+\beta_2X_{i2}+\cdots+\beta_nX_{\text{in}})}{1-\exp(\beta_0+\beta_1X_{i1}+\beta_2X_{i2}+\cdots+\beta_nX_{\text{in}})}. \tag{10}$$

The above equation can be linearly transformed, so

$$\ln\left(\frac{P_i}{1-P_i}\right)=\beta_0+\beta_1X_{i1}+\beta_2X_{i2}+\cdots+\beta_nX_{\text{in}}, i=1,2,\cdots,n. \tag{11}$$

$Y_1, Y_2, \cdots, Y_n$ is an independent binary variable, $f_i(Y_i)$ represents the probability of Yi = 1 or 0. And the likelihood function is

$$L(\beta)=f(Y_1,Y_2,\cdots,Y_n)=\prod_1^nf_i(Y_i)=\prod_1^nP_i^{Y_i}(1-P_i)^{1-Y_i}. \tag{12}$$

Both sides of Formula (12) take the natural logarithm and the log-likelihood function:

$$\ln f(Y_1,Y_2,\cdots,Y_n)=\sum_1^n\left[Y_i\ln\left(\frac{P_i}{1-P_i}\right)\right]+\sum_1^n[\ln(1-P_i)]. \tag{13}$$

Bringing Formula (10) into Formula (13) is

$$\begin{aligned}\ln f(Y_1,Y_2,\cdots,Y_n)&=\sum_1^nY_i(\beta_0+\beta_1X_{i1}+\cdots+\beta_nX_{\text{in}})\\&-\sum_1^n\ln\left[1+e^{(\beta_0+\beta_1X_{i1}+\cdots+\beta_nX_{\text{in}})}\right], i=1,2,\cdots,n.\end{aligned} \tag{14}$$

2.4. Application of Nanomaterial Drug Delivery Carrier in the Treatment of Ophthalmopathy

2.4.1. Application of Nanomaterial Drug Delivery Carrier in the Treatment of Glaucoma. Surgical filtration is a common method of clinical treatment. The main reason is the increase in intraocular pressure caused by conjunctival fibrosis and drainage tract contraction [22, 23]. The advantages are high drug loading and good biocompatibility. Targeted liposome-polypeptide-siRNA nanoparticles as an effective and safe nonviral gene delivery system can be used to prevent conjunctival fibrosis after glaucoma infiltration surgery and other fibroblast-induced ophthalmology.

2.4.2. Application of Drug-Loaded Nanomaterials in Uveitis. Uveitis is a general term for inflammation of the iris, ciliary body, and choroid tissue and is also a chronic inflammation. At present, glucocorticoids, nonsteroidal, anti-inflammatory drugs and immunosuppressive agents can effectively treat uveitis, but these drugs have difficulty reaching the retina to achieve a complete therapeutic effect [24, 25]. Therefore, treating uveitis remains a challenge. Recent studies have shown that nanocells can improve the solubility of drugs and increase the permeability of conjunctival epithelial cells through good hydrophilicity and high drug encapsulation potential.

(1) Application of Drug-Loaded Nanomaterials in Retinal Diseases. By activating specific promoters to reduce the loss of photoreceptor cells, reduce the cavity between the plexus layer and bipolar cells, increase the thickness of the outer nuclear layer of the retina [26, 27], and promote the growth of the retina. And improve the structure of the retina. Therefore, solid lipid nanoparticles gene replacement therapy can restore the retinal structure of mice with retinal protein deficiency.

(2) Application of Nanomaterial Drug Delivery Carrier in the Treatment of Hypertensive Fundus Disease. Through the mutual transformation of the primary and secondary structure of the polypeptide and the self-assembly behavior, among them, polypeptide hydrogel is a self-assembled nanomaterial with nanofiber structure. The hydrogel polypeptide has good biocompatibility and controlled degradation. As a controlled drug delivery system, it has the advantages of high drug loading and smart drug release [28, 29]. Therefore, the gel based on nanofiber polypeptide can prevent the occurrence of hypertensive bottom disease by affecting the proliferation and differentiation of LEC, so as to achieve a better therapeutic effect.

2.5. Drug Delivery Vehicle

2.5.1. Drug Delivery Nanocarrier. With the development of new drug delivery systems, it has become a research hotspot to keep the therapeutic activity of drugs to the maximum while reducing the side effects of drugs. In recent decades, amphiphilic block copolymer drug carriers that can form nanomicelle structures through self-assembly in the water phase have received extensive attention. The amphiphilic block polymer as a drug carrier can physically encapsulate hydrophobic drugs in the core of the micelle, increasing the water solubility of poorly soluble drugs, and the hydrophilic layer formed by the hydrophilic segment of the amphiphilic polymer material can protect the drug carrier from passing through. Pass the biological barrier to enter the diseased site and achieve drug delivery [30, 31]. The chemical composition, molecular weight, and hydrophilic-hydrophobic block ratio of the amphiphilic polymer can be flexibly changed according to the required micelle particle size and morphology. As a drug carrier, nanomicelles can not only extend the time of drug circulation in the body and improve the shortcomings of poor solubility and low stability of the drug but also enrich the drug in the diseased site through the EPR effect and increase the uptake of the drug by cells and tissues.

2.5.2. Characterization of Polymer Materials

(1) NMR Ammonia Spectroscopy. The polymer material was vacuum dried in advance and then analyzed by H-NMR. Weigh 5-10 mg of the sample to be tested and transfer it to a clean NMR tube, add 500 μL of deuterated chloroform or deuterated DMSO to fully dissolve it, use tetramethylsilane as the internal standard, and detect the displacement of ammonia protons in each sample by a nuclear magnetic resonance spectrometer. Analyze the chemical structure of the sample to be tested [32].

(1) Fourier transform infrared spectroscopy

The polymer material is vacuum dried in advance. Take about 200 mg of potassium bromide (KBr) and use a grinding rod to fully grind into ultrafine powder, weigh 2 mg of the sample to be tested and potassium bromide to fully grind and mix, and then make it into potassium bromide tablets for detection by infrared spectroscopy [33–36].

2.5.3. Preparation and Characterization of Micelles

(1) Preparation of Polymer Micelles. The polymer material is prepared by solvent evaporation method to make micelles. The method is briefly described as follows: weigh 10 mg polymer powder and dissolve it in 5 ml tetrahydrofuran, ultrasonically make it fully dissolved, and then add the solution dropwise to 10 ml deionized water at a rate of 1 second/drop through the 21-gauge needle of a glass syringe. During the process, keep the stirring speed at 500 r/min. After the addition is completed, continue to stir until the tetrahydrofuran is fully volatilized to obtain the polymer micelle solution. Before the particle size and morphology of the micelle solution are tested, use a 450 micron filter to filter out impurities and collect it in a container store in a refrigerator at 4°C.

2.5.4. Characterization of the Particle Size and Morphology of Micelles. The dynamic light scattering method is used to detect the average particle size and polydispersity index of the prepared nanomicelles. The abovementioned micelle preparation method is used to prepare a polymer micelle solution with a concentration of 1 mg/ml, and it is detected by a dynamic laser scattering nanoparticle sizer. The test temperature is 25°C. A transmission electron microscope was used to observe the morphology of the prepared nanomicelles. Use the abovementioned micelle preparation method to prepare a nanomicelle solution with a concentration of 1 mg/ml, drop a drop of the micelle solution to be tested on the surface of the carbon film copper mesh, keep it for 90s, absorb the remaining liquid with filter paper, and add a drop of phosphonic acid. (2.5 wt%) aqueous solution for negative dyeing. After dyeing for 60 seconds, the residual dye is absorbed and the surface of the copper mesh is fully evaporated before observation by transmission electron microscope.

3. Experimental Study on the Application of Nanomaterial Drug Delivery System in the Treatment of Hypertensive Fundus Disease

3.1. Test Subject. The main data source of this study is the 120 patients with hypertensive fundus disease who visited the hospital from 2018 to 2020 in X Hospital. These 120 patients with hypertensive fundus disease are the subjects of our study. We obtained the patient's willingness to participate in this study anonymously. The 120 volunteers were divided into groups by random grouping, 60 people in each group. In the experimental group, there were 35 males and 25 females, aged between 37 and 65, with an average age of 44.5 years and a course of 1 year to 3.5 years, with an average of 2.2 years; the control group, 37 males and 23 females, were between 38 and 62 years old, with an average age of about 45.2 years, and the course of disease was 1 to 3 years, with an average of 2 years. The 120 volunteers suffered from hypertensive ocular fundus disease after examination, and

there was no interference from other diseases, and there were no symptoms of drug allergy, and the kidneys and other organs were functioning normally. The three doctors with rich work experience in this hospital are comprehensively judged for judging the degree of treatment. If there is a dispute, the result can be selected through discussion.

3.2. Efficacy Judgment and Index Observation Analysis. The BCVA levels of the patients before treatment, 1 month after treatment, 2 months after treatment, and 3 months after treatment were detected by the eye chart. The BCVA levels of the two groups of patients were compared and statistically recorded. Comparison of the clinical treatment effects of the two groups of patients. According to the degree of recovery of clinical symptoms such as eye pain, swelling, congestion, and the degree of improvement in vision, the level of treatment effect is judged.

3.3. Experimental Method

3.3.1. Preparation Before Treatment. Before treatment, the two groups of patients were tested for vision, and the blood pressure and hemorheology indexes of the two groups of patients were measured at the same time. Provide psychological care to patients, mediate their psychological pressure, and reduce their psychological burden. Try to meet the needs of patients, avoid patients from being left out, and keep patients warm. Introduce the possible reactions of such symptoms to the patient and the cases that have been successfully treated, improve the patient's self-confidence, and help improve the treatment effect.

3.3.2. Treatment. The control group was given low-intensity laser irradiation treatment, using a low-intensity laser with a power of 300 mW to irradiate the eyes of the patient, 2 times/d, 30 min/time, a week as a course of treatment, lasting for two courses; after each irradiation, the patient's eyes were protected by dripping levofloxacin hydrochloride gel. The experimental group was combined with nanotherapy on the basis of the control group. One week was a course of treatment and lasted for two courses. After treatment, the patient's vision, blood pressure, and blood rheology were tested again.

3.4. Gather Data. In order to obtain accurate data to compare and analyze the feasibility and effectiveness of this experiment, this paper uses the Cora dataset and the IMB dataset. The statistical data used in this article has a different unit dimension for each index data. After calculating the data in the previous steps, we can get the similarity between users and select several users closest to the interests and preferences of user u_a to form set N_a. Then, calculate the score of user u_a on j according to the score of the user in the set N_a on the unrated item j, the prediction formula is shown in Formula (15):

$$p_{a,i} = \frac{\sum_{b \in N_a} sim_{u_a,u_b} r_{b,i}}{\sum_{b \in Na} | sim_{u_a,u_b} |}, \tag{15}$$

where $p_{a,i}$ is the predicted score of user a on the unrated item i. In the recommendation system, user scoring preferences are sometimes different. For example, some users are accustomed to giving higher ratings to items, while some are accustomed to giving lower ratings. In order to reduce the difference between users scoring preferences and improve the accuracy of rating prediction, the method of Formula (16) introduces the users average rating $\bar{r}$, and the specific form is shown in Formula (16):

$$p_{a,i} = \overline{r_a} + \frac{\sum_{b \in N_a} sim_{u_a,u_b} (r_{b,i} - \overline{r_b})}{\sum_{b \in N_a} | sim_{u_a,u_b} |}. \tag{16}$$

There are many data standard processing methods, but different data standardization methods will have a certain impact on the evaluation results of the system. For the positive indicator standardization method:

$$y_{ij} = \frac{x_{ij} - \min \{x_{ij}\}}{\max \{x_{ij}\} - \min \{x_{ij}\}}. \tag{17}$$

For negative index standardization methods:

$$y_{ij} = \frac{\max \{x_{ij}\} - x_{ij}}{\max \{x_{ij}\} - \min \{x_{ij}\}}. \tag{18}$$

After standardizing the data, using the principal component analysis of nonlinear logarithmic centering, the processing steps of logarithmic transformation and row vector centering are

$$z_{ij} = \ln y_{ij} - \sum_{i=1}^{m} \ln y_{ij}/m. \tag{19}$$

3.5. Statistical Methods. SPSS23.0 software was used for data processing, and the count data was expressed as a percentage (%), k is the number of data in this experiment, σ^2 is the variance of all survey results, and $P < 0.05$ indicates that the difference is statistically significant. The formula for calculating reliability is shown in equation (20).

$$a = \frac{k}{k-1} \left(1 - \frac{\sum \sigma_i^2}{\sigma^2}\right). \tag{20}$$

4. Experimental Analysis of the Application of Nanomaterial Drug Delivery System in the Treatment of Hypertensive Fundus Disease

4.1. Evaluation Index System Based on Index Reliability Testing. Reliability refers to the stability and reliability of the questionnaire. This article adopts the α coefficient method created by L.J. Cronbach. The α coefficient can be obtained by Reliability Analysis in SPSS software. It is generally believed that the α coefficient above 0.8 indicates that the effect of the index setting is very good, and above 0.7 is also acceptable. Here, we analyze the reliability of each type of object, and the reliability index we choose for each type of object is slightly different. The results are shown in Table 1.

Table 1: Summary Table of Reliability Test Results.

Group	Index combination	Alpha coefficient (α)
Control group	The effect is obvious	0.7932
	Partial relief	
	Stable	
	Invalid	
	Deterioration	
Experimental group	The effect is obvious	0.8226
	Partial relief	
	Stable	
	Invalid	
	Deterioration	

Table 2: Quality of life data analysis table.

	Control group	Test group	Time (t)	Significant difference (P)
0 day	7.832	7.742	0	1
1-2 days	7.952	7.952	0.85	1.202
3-4 days	8.189	8.256	2.132	1.503
5-6 days	8.426	8.628	5.292	2.232
7-8 days	8.827	9.125	8.513	3.273
9-10 days	8.869	9.256	9.952	1.469
11-12 days	8.912	9.389	11.692	0.662
13-14 days	8.982	9.537	13.5	0.001

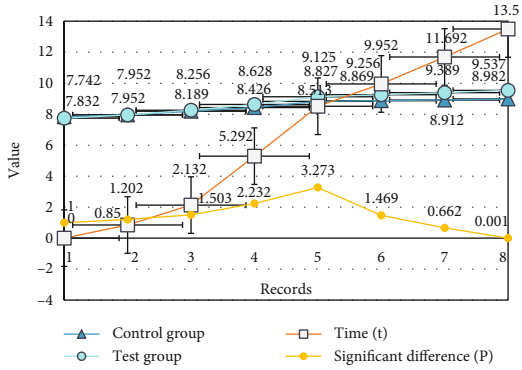

Figure 2: Comparison of the overall quality of life between the two groups of patients before and after intervention.

It can be seen from Table 1 that the influence of the data obtained by the control group and the study group on this experiment is acceptable ($\alpha > 0.7$), and the influence caused by the environment and living habits is within the acceptable range, satisfying the experiment prerequisites to start.

4.2. Based on the Quality of Life and Complications of the Two Groups of Patients during Treatment

4.2.1. Comparative Analysis of the Quality of Life of the Two Groups of Patients. We first compare and analyze the quality of life of the two groups of patients. We choose to conduct surveys and process data for analysis every two days before treatment. When we conduct data collection and analysis, we ask three doctors with extensive work experience to participate in this experiment, the overall quality of life of the patients was comprehensively scored to calculate the significant difference, and the results are shown in Table 2. We make a scatter plot based on this result, as shown in Figure 2.

It can be seen from Figure 2 that there was no difference in the overall quality of life of the two groups before the treatment and at the end of the first course of treatment ($P > 0.05$), until the end of the second course of treatment, the overall quality of life of the experimental group was higher than that of the control group ($P < 0.05$). That is to say, when the treatment is completed, the overall life treatment of the experimental group is higher than that of the control group. This conclusion is reliable and there is no significant difference.

Table 3: Anxiety data analysis table.

	Control group	Test group	Time (t)	Significant difference (P)
0 day	17.000	17.000	0.074	0.984
1-2 days	15.521	15.387	0.241	0.821
3-4 days	14.127	13.124	1.121	0.234
5-6 days	12.682	11.486	2.012	0.112
7-8 days	11.020	9.264	2.982	0.004
9-10 days	8.869	7.132	3.125	0.003
11-12 days	6.852	4.162	3.632	0.002
13-14 days	3.326	1.521	4.437	0.001

4.2.2. Comparative Analysis of Anxiety Degree between Two Groups. We compare and analyze the anxiety of the two groups of patients. We choose to conduct surveys and process data for analysis every two days before treatment. When we conduct data collection and analysis, we asked three doctors with extensive work experience participating in this experiment, the patients' anxiety level was comprehensively scored to calculate the significant difference, and the results are shown in Table 3. We make a bar graph based on this result, as shown in Figure 3.

It can be seen from Figure 3 that there was no difference in anxiety between the two groups of patients before the first use of targeted drugs ($P > 0.05$). The two groups of patients were compared at the end of the first course of treatment and at the end of the second course of treatment. The score of the experimental group was low. Compared with the control group ($P < 0.05$), that is to say, the anxiety level of the experimental group is lower than that of the control group during half of the treatment. This conclusion is reliable and there is no significant difference.

4.2.3. Comparative Analysis of Depression Degree of Two Groups of Patients. We made a comparative analysis of the depression levels of the two groups of patients. We chose to conduct surveys and process data for analysis every two days before treatment. When we collected and analyzed data, we asked the three doctors who participated in this experiment with extensive work experience, the degree of

depression of the patients was comprehensively scored to calculate the significant difference, and the results are shown in Table 4. We make a line chart based on this result, as shown in Figure 4.

It can be seen from Table 4 that there was no difference in the degree of depression between the two groups of patients before the first use of targeted drugs and at the end of the first course of treatment ($P > 0.05$), and until the end of the second course of treatment, the degree of depression in the experimental group was higher than that in the control group ($P < 0.05$). That is to say, the degree of depression in the experimental group is higher than that in the control group when the treatment is completed. This conclusion is reliable and there is no significant difference.

4.3. Based on Single-Factor Comparison. First, through univariate analysis, all the above possible factors are studied to initially screen out the relevant factors. Among them, the chi-square test is used for categorical factors, and the independent sample T test is used for data factors. The results are shown in Table 5.

(1) Analyze the treatment effects of different genders

We analyzed the treatment effect of patients according to different gender groups at the same time and judged the treatment effect level according to the degree of recovery of clinical symptoms such as eye pain, swelling, congestion, and the degree of improvement in vision. Let the three doctors with extensive work experience participating in this experiment calculate the significant difference by comprehensively scoring the patient's overall quality of life, as shown in Figure 5.

It can be seen from Figure 5 that the cure rate for men is 93.05%, and the cure rate for women is 89.58%. At the same time, whether it is completely cured or completely ineffective, there is no correlation between gender and ERD ($P > 0.05$). That is to say, the probability of suffering from hypertensive fundus disease is not related to gender. This conclusion is reliable and there is no significant difference.

4.3.1. Analyze According to whether Cataract Surgery Has Been Done. We divided patients into groups according to whether they had undergone cataract surgery and analyzed their treatment effects. We judged the level of treatment effect according to the degree of recovery of clinical symptoms such as eye pain, swelling, and congestion, and the degree of improvement in vision. Let the three doctors with extensive work experience participating in this experiment calculate the significant difference by comprehensively scoring the patient's overall quality of life, as shown in Figure 6.

It can be seen from Figure 6 that the cure rate of patients who have undergone cataract surgery is 83.33%, and the cure rate of patients who have not undergone cataract surgery is 91.22%. At the same time, whether it is completely cured or completely ineffective, gender is related to the occurrence of ERD. Sex ($P < 0.05$). That is to say, the probability of suffering from hypertensive fundus disease is related to whether

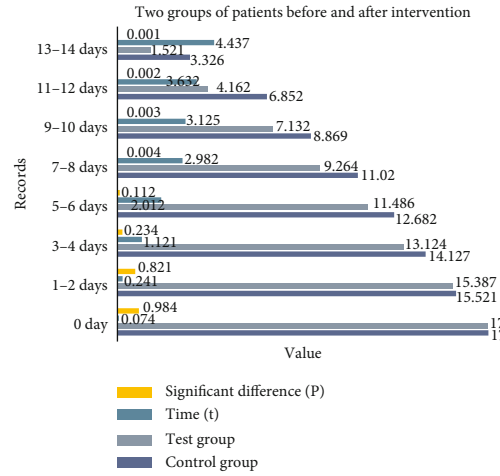

Figure 3: Comparison of anxiety between the two groups of patients before and after intervention.

Table 4: Depression data analysis table.

	Control group	Test group	Time (t)	Significant difference (P)
0 day	7.00	6.98	0.044	0.984
1-2 days	6.33	6.40	0.489	0.922
3-4 days	5.35	5.12	1.121	0.552
5-6 days	3.98	3.87	1.428	0.213
7-8 days	3.42	2.39	1.818	0.073
9-10 days	2.55	2.10	1.321	0.182
11-12 days	2.09	1.82	0.992	0.289
13-14 days	1.66	1.41	0.776	0.44

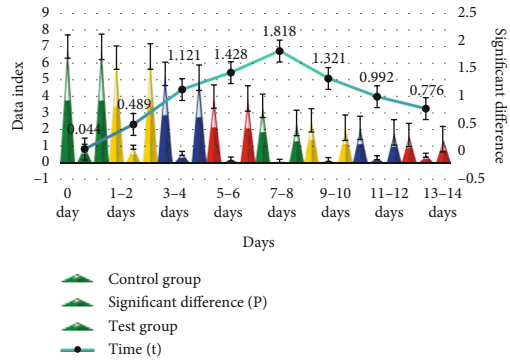

Figure 4: Comparison of depression between two groups of patients before and after intervention.

or not cataract surgery has been done. This conclusion is reliable and there are significant differences.

4.3.2. Analyze According to whether PRP Surgery Has Been Done. We grouped patients according to whether they had undergone PRP surgery and analyzed their treatment effects at the same time. According to the degree of recovery of clinical symptoms such as eye pain, swelling, congestion, and the degree of improvement in vision, the level of treatment

Table 5: Categorical independent variable and dependent variable assignment table.

Assignment variable		Category	Number	Proportion
Dependent variable	Result	ERD	10	8.3%
		NO ERD	110	91.7%
Independent variable	Gender	Male	72	60%
		Female	48	40%
	History of cataract surgery	Yes	6	5%
		No	114	95%
	PRP treatment history	Yes	22	18.3%
		No	98	81.7%
	History of anti-VEGF treatment before surgery	Yes	30	25%
		No	90	75%

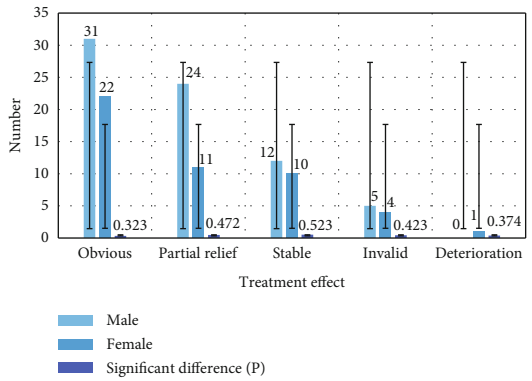

Figure 5: Analyze the treatment effect of different genders.

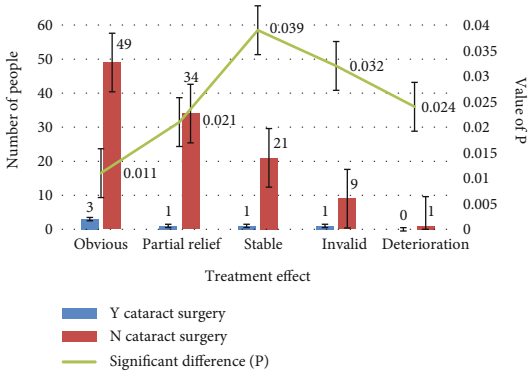

Figure 6: Analysis diagram of environmental pollution caused by three kinds of cars driving the same distance.

effect was evaluated. Let the three doctors with extensive work experience participating in this experiment calculate the significant difference by comprehensively scoring the patient's overall quality of life, as shown in Figure 7.

It can be seen from Figure 7 that the cure rate of patients who have undergone PRP surgery is 86.36%, and the cure rate of patients who have not undergone cataract surgery is 92.85%. At the same time, whether it is completely cured or completely ineffective, there is no correlation between gender and ERD. Sex ($P > 0.05$). That is to say, the probability of suffering from hypertensive fundus disease has nothing to do with whether or not PRP has been performed. This conclusion is reliable and there is no significant difference. Because it is impossible to count the number of treatment points of patients undergoing PRP before surgery in this study, this may have a certain impact on this result.

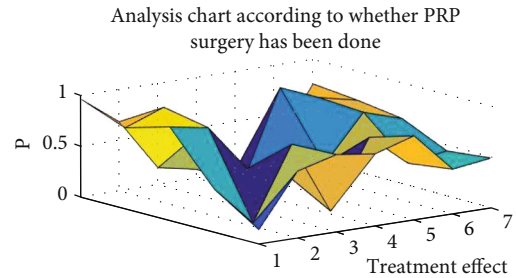

Figure 7: Analysis chart according to whether PRP surgery has been done.

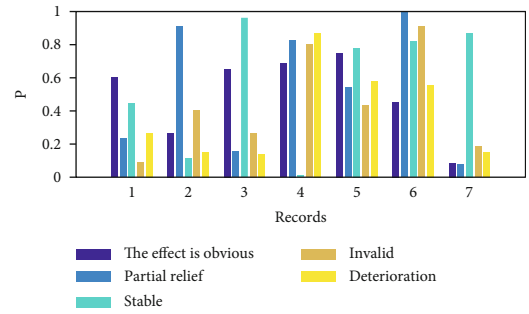

Figure 8: According to whether there is a history of anti-VEGF treatment before surgery.

4.3.3. Analyze According to whether There Is a History of Anti-VEGF Treatment before Surgery. We grouped patients according to whether they had a history of anti-VEGF treatment before surgery and analyzed their treatment effects. We judged the treatment effect according to the degree of recovery of clinical symptoms such as eye pain, swelling, and congestion, and the degree of visual improvement. Let the three doctors with extensive work experience participating in this experiment calculate the significant difference by comprehensively scoring the patient's overall quality of life, as shown in Figure 8.

It can be seen from Figure 8 whether the cure rate of patients with a history of preoperative anti-VEGF therapy is 90%, and the cure rate of patients who have not undergone cataract surgery is 92.22%. At the same time, whether it is completely cured or completely ineffective, it is all gender and ERD. There is a correlation ($P < 0.05$). That is to say, the probability of suffering from hypertensive fundus disease is related to whether there is a history of anti-VEGF treatment before operation. This conclusion is reliable and there are significant differences. In this study, due to the fact that there are many new blood vessels in the fundus of some patients, in order to smooth the operation and achieve better results after the operation and reduce the occurrence of rebleeding, anti-VEGF treatment is used within 3-7 days before the operation, and the drug is selected according to the patient's own wishes. All patients in this group who received anti-VEGF treatment before surgery did not develop ERD.

5. Conclusion

The use of nanocarriers for drug delivery can significantly improve the bioavailability of the drug, reduce the dosage and frequency of administration, increase the residence time of the drug in the local tissue, and reduce the side effects of the drug, overcoming many of its shortcomings. Traditional methods of administration can improve ocular tissue disease. At present, the ophthalmic drug delivery system is still in the process of continuous improvement. Therefore, it is a huge challenge to develop a drug delivery system for the back of the eye that results in a sustained and controlled release, is noninvasive, and can be self-administered by the patient. Advances in nanodrug delivery systems and drug delivery technologies have greatly promoted the development of ophthalmic drug delivery and provided broad prospects for the treatment of ophthalmic diseases. However, there are few reports on the quality control and safety assessment of the drug distribution system, so further research and exploration are needed. It is believed that with the continuous deepening of related research, nanodrug delivery systems will be more used in clinical treatment during the administration of ophthalmic drugs, which will bring good news to patients with ophthalmological diseases.

At present, most retinal blood vessel extraction methods are mainly used for normal retinal images. Therefore, when applied to a large range of lesion images, it is difficult to accurately extract blood vessels due to the interference of lesions and other nonvascular structures, and a large number of nonvascular structures cannot be filtered. In addition, this article focuses on vascular bone extraction and vascular structure segmentation methods suitable for retinal imaging. At the same time, in order to further eliminate the residual nonvascular pixels, a multiple hysteresis threshold method based on dilution of the standard hysteresis threshold is proposed. On this basis, a method suitable for fundus was proposed. The method of extracting the vascular skeleton of the nonvascular structure of the diseased image is suppressed. This method filters the nonvascular structures in the patient image to a large extent and can keep the blood vessel skeleton relatively complete.

This study investigated the effect of the combination of low-intensity laser radiation and traditional Chinese medicine treatment on hematological indicators of patients with hypertension. It can be seen from the results that at different times after treatment, the BCVA of the study group was significantly higher than that of the control group. Recovering vision can obviously help. In the treatment process, the combined treatment of the two methods did not increase the incidence of side effects but reduced the incidence of side effects. At the same time, the results of the two bleeding groups showed that the bleeding index of the study group was better than that of the control group. The treatment effect is ideal. In addition, doctors must continue to strengthen research to provide patients with more effective treatment methods and drugs to accelerate the recovery of vision.

Although the use of MPEG-PCL nanomicelle ocular drug delivery carrier has carried out in-depth research on the treatment of hypertensive fundus diseases, there are still many shortcomings. The depth and breadth of this research are not enough. In the process of this research, the experimental data, the selection and acquisition of the test were carried out under absolutely ideal conditions, and the completeness and effectiveness were not enough. Some interfering factors involved in the experiment were not taken into account, and the patient's condition tracking was also restricted by many factors. The research on the academic level is also limited, and the treatment of hypertensive fundus diseases is still in the preliminary stage. In the future work, appropriate treatment methods and means will be studied from more perspectives based on the existing technology and level, and the quality of medical treatment will be continuously improved.

Data Availability

The data that support the findings of this study are available from the corresponding author upon reasonable request.

Conflicts of Interest

The authors declared no potential conflicts of interest with respect to the research, authorship, and/or publication of this article.

Acknowledgments

This work was supported by the Key Fund of Department of Cardiology, Shandong University Qilu Hospital (Qingdao) (QDKY2019ZD04), People's Livelihood Science and Technology Project of Qingdao (Application of DEEPVESSEL FFR in coronary artery heart disease complicated with diabetes mellitus), and Qingdao Key Health Discipline Development Fund.

References

[1] H. Wei, A. Sehgal, and N. Kehtarnavaz, "A deep learning-based smartphone app for real-time detection of retinal abnormalities in fundus images," *Real-Time Image Processing and Deep Learning*, vol. 10996, 2019.

[2] K. Shankar, Y. Zhang, Y. Liu, L. Wu, and C. H. Chen, "Hyperparameter tuning deep learning for diabetic retinopathy fundus image classification," *Access*, vol. 8, pp. 118164–118173, 2020.

[3] W. Fengping and W. Weixing, "Road extraction using modified dark channel prior and neighborhood FCM in foggy aerial images," *Multimedia Tools and Applications*, vol. 78, no. 1, pp. 947–964, 2019.

[4] R. Geetha Ramani and L. Balasubramanian, "Retinal blood vessel segmentation employing image processing and data mining techniques for computerized retinal image analysis," *Engineering*, vol. 36, no. 1, pp. 102–118, 2016.

[5] L. C. Rodrigues and M. Marengoni, "Segmentation of optic disc and blood vessels in retinal images using wavelets, mathematical morphology and Hessian-based multi-scale filtering," *Biomedical Signal Processing & Control*, vol. 36, pp. 39–49, 2017.

[6] Y. Zhang, L. Sun, H. Song, and X. Cao, "Ubiquitous WSN for healthcare: recent advances and future prospects," *IEEE Internet of Things Journal*, vol. 1, no. 4, pp. 311–318, 2014.

[7] J. Choi, C. Choi, S. Kim, and H. Ko, "Medical Information Protection Frameworks for Smart Healthcare based on IoT," in *Proceedings of the 9th International Conference on Web Intelligence, Mining and Semantics (WIMS 2019)*, pp. 1–5, Seoul, Korea, 2019.

[8] Z. Lv and H. Ko, "Introduction to the special issue on recent trends in medical data security for e-health applications," *ACM Transactions on Multimidia Computing Communications and Applications*, vol. 17, 2021.

[9] A. K. Singh, A. Anand, Z. Lv, H. Ko, and A. Mohan, "A survey on healthcare data: a security perspective," *ACM Transactions on Multimedia Computing Communications and Applications*, vol. 17, no. 2s, pp. 1–26, 2021.

[10] C. Haythornthwaite, "Learning, connectivity and networks," *New Library World*, vol. 120, no. 1/2, pp. 19–38, 2019.

[11] M. Zhang, X. Cao, L. Peng, and R. Niu, "Landslide susceptibility mapping based on global and local logistic regression models in Three Gorges Reservoir area, China," *Environmental Earth Sciences*, vol. 75, no. 11, pp. 1–11, 2016.

[12] R. Takahashi, Y. Hatanaka, T. Nakagawa et al., "Automated analysis of blood vessel intersections in retinal images for diagnosis of hypertension," *Medical Imaging Technology*, vol. 24, no. 4, pp. 270–276, 2016.

[13] J. D. Benck, T. R. Hellstern, J. Kibsgaard, P. Chakthranont, and T. F. Jaramillo, "Catalyzing the hydrogen evolution reaction (HER) with molybdenum sulfide nanomaterials," *ACS Catalysis*, vol. 4, no. 11, pp. 3957–3971, 2014.

[14] J. O. Tijani, O. O. Fatoba, O. O. Babajide, and L. F. Petrik, "Pharmaceuticals, endocrine disruptors, personal care products, nanomaterials and perfluorinated pollutants: a review," *Environmental Chemistry Letters*, vol. 14, no. 1, pp. 27–49, 2016.

[15] K. Rasmussen, M. González, P. Kearns, J. R. Sintes, F. Rossi, and P. Sayre, "Review of achievements of the OECD working party on manufactured nanomaterials' testing and assessment programme. From exploratory testing to test guidelines," *Regulatory Toxicology and Pharmacology*, vol. 74, no. 11, pp. 147–160, 2016.

[16] M. Hu, Z. Yao, and X. Wang, "Graphene-based nanomaterials for catalysis," *Industrial & Engineering Chemistry Research*, vol. 56, no. 13, pp. 3477–3502, 2017.

[17] D. Bozyigit, N. Yazdani, M. Yarema et al., "Soft surfaces of nanomaterials enable strong phonon interactions," *Nature*, vol. 531, no. 7596, pp. 618–622, 2016.

[18] K. Garner, S. Suh, and A. A. Keller, "Response to comments on "assessing the risk of engineered nanomaterials in the environment: development and application of the nanoFate Model"," *Environmental Science & Technology*, vol. 52, no. 9, pp. 5511–5511, 2018.

[19] N. B. Raja, I. Çiçek, N. Türkoğlu, O. Aydin, and A. Kawasaki, "Correction to: landslide susceptibility mapping of the Sera River Basin using logistic regression model," *Natural Hazards*, vol. 91, no. 3, pp. 1423–1423, 2018.

[20] L. Jianfeng, L. Zhiyong, Z. Yan, Z. Wei, and G. Maolong, "Analysis of factors affecting the prognosis of ICU patients by multiple logistic regression model: a retrospective cohort study of 1 299 patients in 12 consecutive years," *Zhonghua wei Zhong Bing ji jiu yi xue*, vol. 29, no. 7, pp. 602–607, 2017.

[21] L. Y. Sun, C. L. Miao, and L. Yang, "Ecological environmental early-warning model for strategic emerging industries in China based on logistic regression," *Ecological Indicators*, vol. 84, no. JAN., pp. 748–752, 2018.

[22] L. Essa, D. Laughton, and J. S. Wolffsohn, "Can the optimum artificial tear treatment for dry eye disease be predicted from presenting signs and symptoms?," *Contact Lens and Anterior Eye*, vol. 41, no. 1, pp. 60–68, 2018.

[23] J. Qian, "The stepwise establishment of standardized treatment for the thyroid eye disease," *Zhonghua Yan Ke Za Zhi*, vol. 53, no. 6, pp. 404–407, 2017.

[24] S. Fraser-Bell, R. Symes, and A. Vaze, "Hypertensive eye disease: a review," *Clinical & Experimental Ophthalmology*, vol. 45, no. 1, pp. 45–53, 2017.

[25] S. Jun, "Definition and diagnostic criteria of dry eye disease: historical overview and future directions," *Investigative Ophthalmology & Visual Science*, vol. 59, no. 14, pp. DES7–DES12, 2018.

[26] N. Itoh, E. Yamamoto, T. Santa, T. Funatsu, and M. Kato, "Effect of nanoparticle surface on the HPLC elution profile of liposomal nanoparticles," *Pharmaceutical Research*, vol. 33, no. 6, pp. 1440–1446, 2016.

[27] P. L. Lam, W. Y. Wong, Z. Bian, C. H. Chui, and R. Gambari, "Recent advances in green nanoparticulate systems for drug delivery: efficient delivery and safety concern," *Nanomedicine*, vol. 12, no. 4, pp. 357–385, 2017.

[28] A. C. Fortes, V. D. N. Bezzon, G. L. B. de Araújo, C. O. P. Santos, and H. G. Ferraz, "Preparation and physicochemical characterization of drug loaded in castor oil-based polyurethane," *Journal of Thermal Analysis and Calorimetry*, vol. 139, no. 3, pp. 1949–1957, 2020.

[29] J. Zhou, S. Chen, P. Luo, B. Du, and H. Yao, "A "submunition" dual-drug system based on smart hollow NaYF4/apoferritin nanocage for upconversion imaging," *RSC Advances*, vol. 6, no. 40, pp. 33443–33454, 2016.

[30] V. Agrahari, V. Agrahari, and A. K. Mitra, "Nanocarrier fabrication and macromolecule drug delivery: challenges and opportunities," *Therapeutic Delivery*, vol. 7, no. 4, pp. 257–278, 2016.

[31] Q. B. Wang and X. L. Wang, "Advances in designation of targeting nanocarrier-drug delivery systems for pancreatic cancer. Fudan University," *Journal of Medical Sciences*, vol. 45, no. 1, 2018.

[32] T. Buttersack, P. E. Mason, R. S. McMullen et al., "Valence and core-level X-ray photoelectron spectroscopy of a liquid ammonia microjet," *Journal of the American Chemical Society*, vol. 141, no. 5, pp. 1838–1841, 2019.

[33] S. H. Eom, S. Senthilarasu, P. Uthirakumar et al., "Preparation and characterization of nano-scale ZnO as a buffer layer for inkjet printing of silver cathode in polymer solar cells," *Solar Energy Materials & Solar Cells*, vol. 92, no. 5, pp. 564–570, 2008.

[34] A. K. Sood, Pritambir, and M. Aggarwal, "A mathematical approach to a more accurate determination of critical micelle concentration and other thermodynamic parameters of 14-2-14 gemini surfactant in water–organic solvent mixed media at variable temperatures," *Journal of Surfactants and Detergents*, vol. 20, no. 1, pp. 297–305, 2017.

[35] S. Wang and K. Zhao, "Dielectric analysis for the spherical and rodlike micelle aggregates formed from a gemini surfactant: driving forces of micellization and stability of micelles," *Langmuir*, vol. 32, no. 30, pp. 7530–7540, 2016.

[36] B. Xue and Z. Wu, "Key technologies of steel plate surface defect detection system based on artificial intelligence machine vision," *Wireless Communications and Mobile Computing*, vol. 2021, Article ID 5553470, 12 pages, 2021.